Proceedings of the International Conference on Isochronous Cyclotrons, Gatlinburg, Tennessee, 1966

HEAVY ION INJECTION FOR STRIPPING IN THE CENTRAL REGION OF THE CEVIL.

C. Bieth, A. Cabrespine, Ch. Goldstein.

Nuclear Physics Institute, Orsay, France

Abstract

We plan to inject a heavy ions beam, previously accelerated, into the median plane of the Orsay CEVIL. The heavily charged ions, obtained after the stripping operation in the central region of the cyclotron, can achieve an energy proportional to the square of the charge number.

The choice of injection energy represents, in fact, a compromise between price and performance. The e/m ratio, chosen to be $\geq 0{,}1$, will give the possibility of accelerating heavy ions up to bromine, and Krypton.

The injector will be a linear accelerator, either pulsed or continuous. The distance between the linear accelerator and the cyclotron will allow the debunching of beam packets, at the RF frequency (25 Mc/s).

The drift tube circuit is similar to the Manchester one. We have gone duply into the problem of the focusing system in order to obtain an accelerated beam of more than 100 μA.

The chosen solution was strong focusing grids, obtained by means of two parallel tungsten strips placed at the beginning of each drift tube, each pair being at 90° to the preceeding one.

The theoretical studies of this apparatus are well advanced at present ; the industrial production of the main elements is under way. The whole equipment should be completely finished in July 1967.

Introduction

The CEVIL can accelerate heavy multicharged ions to a maximal energy proportional to the square of the charge number and inversely proportional to its atomic mass :

$$E\ (MeV) = 70\ Zi^2/A$$

To reach high energies necessary for nuclear reactions, it is then interesting to accelerate ions as charged as possible, more specially as the considered ions' atomic masses increase[1].

Now the heavy ion sources give at the utmost ions, the charge rate of which is 5 or 6 in $Z < 30$ region. If these charge rates are to be increased it is necessary to use stripping of heavy previously accelerated ions through a thin foil. The charge distribution depends then on the incident velocity of the ions and shifts towards high charges when velocity increases. This leads to contemplate injecting into the CEVIL previously accelerated ions, stripping then in the central region of the cyclotron, then accelerating them in the cyclotronic range. This idea is not a recent one as it was suggested by Tobias[2] in 1952. After having seriously studied the possibilities of various types of injection accelerators we chose to use a linear accelerator.

Determination of the linear accelerator's main-parameters

The essentiel part of the linear accelerator project is the wish to obtain a continuous ion beam, incidentally pulsed for the greater masses. In fact the radio-frequency power necessary to reach the required accelerating voltage cannot generally be given in continious operating over 30 MHz. We are then brought to abandon the so-called Alvarez structure, the volume and power of which become prohibitive, in favour of a better-fit structure as far as low frequencies are concerned. The quarter-wave resonant lines, very often used in the cyclotrons are still suitable to the studied region.

Calculations in various coaxial or twin-lined structures carried out by means of the method followed by the CEVIL[3] showed that combination of twin-lined resonant quarter-waves, already used in Manchester[4], had a greater shunt

impedance (fig.1). More thorough investigations allowed to find the best sizes the wires and outer conductor should be given, as a function of the radio-frequency power[5].

Injection energy

The energy of the incident beam should be chosen by considering the results on stripping experiments and the charge distribution necessary for the CEVIL caracteristics. As a first consideration the Lassen's suggestion[6] seems to indicate that the average charge state of stripped ions is proportional to the square root of the velocity. Furthermore the known results show that, for a given energy the more probable charge state is proportional to the square root of the mass.

These results are shown in Fig. 2 and the maximum energy obtained for various injection energy is shown in fig.3.

Choice of the Zi/A ratio and of the ion source.

As the linear accelerator admits all particles the Zi/A ratio of which is equal or greater than the value determined by the chosen maximum electric field, we must point out that :

a) the cost price increases when $\frac{Zi}{A}$ decreases
b) the ion sources cannot provide all required ions if $\frac{Zi}{A}$ increases, as shown in table III.

Consequently an $\frac{Zi}{A} \geq 0{,}1$ was chosen, which requires an acceleration > 10 MV. The ion source will be identical to that of Dubna[7]. It will be in continuous operating up to masses 30 and 40 then in pulsed operating up to masses 80. It is quite useful to recall that the power requirements of such a source, including focusing and analysis parts, can reach 100 kVA, which slightly conditions the preaccelerating voltage.

Injection Velocity

Once these main parameters had been selected, nearly all others follow from them. Since our structure accelerating mode, allows accelerating on the mode $L = \frac{\beta\lambda}{2}$, the repeating lenght can be expressed as $L = \frac{1}{2f}\sqrt{\frac{2e}{m}}\,(V_o + V_{RF}\, T \cos\phi_S)$.

The two values to be now settled are :

a) accelerating voltage V_o
b) maximum voltage in the gap depending on the maximum permissible electric field.

The standing choice of ratio gap lenght over repeating lenght is $\frac{1}{4}$ in $L = \beta\lambda$ mode and $\frac{1}{2}$ in $\frac{\beta\lambda}{2}$ mode. For an equal maximum electric field our accelerator can be compared with that of Berkeley or Yale[8] for instance. The 25 MHz frequency chosen (instead of 70 MHz) increases the repeating lenght by a factor 2.8. The latter can be reduced by 1.22 by chosing $Zi/A = 0.1$ (instead of 0.15). For a same repeating lenght the preaccelerating voltage V_o can be reduced by a factor approximately equal to five, that is 100 kV instead of 500 kV. This reduction offers us a twofold advantage :

a) in this voltage region large current-flow supplies can be found (several 10 mA)
b) the power requirements needed by the source (∿ 100 KVA) at a 100 KV voltage can be provided by means of a mere insulation transformer the losses of which may even become significant.

We finally chose a SAMES high-stability power supply 140 kV, 14 mA. The repeating lenght gain, remaining so, allows ratio g/L to vary at the machine entrance. With for instance $g/L = \frac{1}{2}$ phase acceptance is noticeably increased as we shall see further.

Accelerating cavity

We already gave the outlines of the structure type chosen. Fig.5 shows a transversal section of the cavity at a short-circuit level. The calculated voltage distribution (Fig.6) shows that this structure type can also increase voltage according to a law such that the electric field is maximum at full lenght of the machine. We must also point that the general mechanical tolerance on the electrodes is low, since only interelectrode capacities modify the frequency resonance. If we compare ours with the Berkeley and Yale accelerators that give 6.7 MV for 400 KW, we obtain 11.6 MV for 240 KW, which shows the improvement we brought.

Main characteristics follow :

Final energy : 1.16 MeV/nucléon
Resonance frequency: 25 MHz
4 associated quarter-waves : Total length 10 m
4 adjustable short-circuits.
Maximum peak voltage : 130 KV input , 500 KV output
Structure maximum power : 240 KW (for $\frac{e}{m} = 0.1$)
drift tubes number : 56
Effective shunt impedance : 60 MΩ/m
Overvoltage coeffient : Q = 6000
Cavity vacuum : two 15,000 l/sec oils

pumps with refrigerated bafle or turbomolecular pump.

Radiofrequency emitter : CFTH amplifier of 250 KW for continuous operating and 400 KW for pulse operating, with pulse duration ranging from 0.8 to 2,5 ms and repetition periods from 2 to 16 ms. Cavity coupling : by 75Ω feeder and controlled coupling loop.

Determination of the electrodes in this structure type sets quite a few problems all connected to each other.

a) Electrodes can be determined only after having obtained accurate voltage distribution along the machine. The latter is also modified by the lenght of electrodes. We then built a quarter-scale model (Fig.7) and after three consecutive electrode sets, we obtained with satisfying accuracy an agreement between calculations and measurements. Voltage distribution measurements were carried out by means of the perturbation method. (with a metal ball 3 to 4 mm diameter)[5]. A recording system could give quickly all the ensemble field curve (Fig.8) and, by a planimeter integration, the potential value, for the considered gap.

b) The stable phase angle φ_s, the time of flight, in each gap, the maximum electric fields on the electrode-outlines, the beam passage-diameter, etc. must be previously determined.

We also made sure on the model that we actually obtained the calculated overvoltage value Q = 3000 (that gives 6000 on true scale). We are now carrying on our investigations on the emitter coupling.

Focusing system

A few years ago, this section would have been quite short ; indeed,after having chosen such a low preaccelerating voltage and a continuous beam, strong focusing by magnetic quadrupole inside the electrodes cannot be used at all, because of the magnetic field values that must be obtained and subsequently of the powers to be pumped out. And, as in Berkeley, Yale or Manchester we would have chosen right away grid-focusing, by making the same shapes as on those machines.

Nowadays, various suggestions or investigations have been put forward. All are based on the use of the electric field itself to obtain focusing, which, except alternating-phase focusing, leads to abandon the cylindrical character of the electric field in the gap.

This can be realized by means of rectangular boxes crossed at 90° [9] , or by fitting the electrode ends with fingers[10].

To obtain with these various devices phase acceptance identical to that of the grid in Berkeley, the ratio $\frac{g}{L}$ must be considerably reduced so as to tend to $\frac{1}{8}$ to $\frac{1}{10}$. Of course, because of breakdowns, this leads to reduce the accelerating rate by meter, which can then hardly be greater than 0.5 to 0.8 MV/m, which increases the machine lenght by a factor 1.5 to 2.

Informed by these investigations, we went back, as Lapostolle suggested, to the grid focusing, by trying to obtain different field dissymetries in two perpendicular planes. We could indeed conceive that two parallel bands would give a strong focusing effect similar to that of the rectangular boxes, only if the wires stood at 90° from each other, between two consecutive electrodes (Fig.9). In order to obtain comparable results we carried out in the electrolytic tank measurements on the old Berkeley grids, the detailed results of which we knew well[11] (Fig.10).

Let us recall briefly the method used by Smith and Gluckstern.

The movement equation is in x or y plan :

$$m \frac{dv_x}{dt} = eEx = -e\frac{\delta V_x}{\delta x} = -e\frac{\delta Vo(x)}{\delta x}\cos\left(\frac{2\pi z}{L} + \phi\right)$$

where $Vx = Vo(x) \cos\left(\frac{2\pi z}{L} + \phi\right)$ and z the beam direction.

$$\Delta v_x = -\frac{e}{m}\int \frac{\delta Vo(x)}{\delta x} \cos\left(\frac{2\pi z}{L} + \phi\right) dt$$

if we assume v_z = Cte in the gap. The radial impulse

$$\Delta v_x = \frac{-e}{m v_z}\int \frac{\delta Vo(x)}{\delta x} \cos\left(\frac{2\pi z}{L} + \phi\right) dz$$

with : $$\frac{\delta S}{\delta x}(x,o) = \frac{-1}{\Delta V}\int_{-\infty}^{+\infty} \frac{\delta Vo(x)}{\delta x}\cos\frac{2\pi z}{L} d\left(\frac{2\pi z}{L}\right)$$

and $$\frac{\delta C}{\delta x}(x,o) = \frac{1}{\Delta V}\int_{-\infty}^{+\infty} \frac{\delta V_o(x)}{\delta x}\sin\frac{2\pi z}{L}\, d\left(\frac{2\pi z}{L}\right)$$

the radial impulse becomes :

$$\Delta v_x = \frac{e}{m v_z}.\Delta V.\frac{L}{2\pi}\left(\frac{\delta S}{\delta x}\cos\phi - \frac{\delta C}{\delta x}\sin\phi\right)$$

which is the same in the y plan but with S' and C'. If the radial impulse is small the radial motion can be described after two gaps by two radial impulse, but with S and S' and C and C' because grids are oriented at 90° from each other :

$$\frac{1}{2} m x'^2 = \frac{e\Delta V}{2\pi}\{(S+S')\cos\phi - (C+C')\sin\phi\}$$

Phases will lead to stable motion can be obtained by this equation and on the curves on fig.11 and 12, the results can be analysed, it seems that we can normally choose ϕ_S = - 20°. In spite of simplifi-

cation brought to the calculations, constant velocity, constant radius etc... results of measurements carried out in Berkeley show that the synchronism phase is close to the calculated one. However, since we have in Orsay a computing center equipped with UNIVAC at our disponal, we can now make a computing program point by point from the equipotential lines measured for various values of ratios g/L and g/a.

It is also interesting to compare the transparency obtained with this type of grid with the one from Berkeley. Curves on fig.13 show that we can be sure of a transparency gain. Besides, we tried to improve the maximum possible dissipation power on the grids. When constant-width grids are abandoned in favour of variable-width grids as shown fig.14, the temperature for a same power can be considerably reduced without increasing apparent transparency, even with a real beam since this is the low-density current region, the central part stays unchanged). We must point out that on fig.14 bis the grids are actually cut in their middles to avoid warping due to the dilatation.

With this type of grid we drawed the total shadowing effect as a function of the gap number, still assuming that the beam filled in electrode passage opening. (Fig.15).

We may then think that the transparency efficiency could reach 50 %, without considering alignment defects, etc... Fig. 16 shows such a grid, realized by the CSF from tungsten band on a nickel holder rebrazed on the electrode nosepiece, the linear accelerator efficiency could then be :

injection efficiency : $\frac{3\phi_s}{2\pi}$ = 16 %

- with buncher : 40 %
- Total efficiency = 20 %

Beam injection into the CEVIL

A fast calculation was performed to determine the input beam path into the CEV and junction with the cyclotron paths after stripping[12]. Fig. 17 shows these paths for $Zi/A \geq 0.1$, and a magnetic field value equal to 14 Kgauss. A complete computing program is now being carried out to determine accurate paths and focusing conditions.

A plan view of Hilae injector and CEVIL is shown in fig. 18.

References

1. A. Cabrespine Internal Report mars 1964
2. Tobias Phys. Rev. 85 764 (1952)
3. A. Cabrespine, Y. Dupuis, C. Bieth CERN 63-19 256 (1963)
4. G. Massibian, J.R. Bennett, D. Broadbent, S. Devons, R.W.R. Hoisengton and V.E. Miller Rev. Scient. Inst. 32, 1316 (1961)
5. J. Bosser CNAM Thesis (1966)
6. Lassen Phys. Rev. 69 137 (1946)
7. P.M. Morosov, Makov, Joffe Atom. Energy 3, 272 (1957)
8. E.L. Hubbard, W.R. Baker, K.W. Ehlers, H.S Gordon, R.M. Main N.J. Morris, R. Peters, L. Smith, C.M. Van Atta, and F. Voelker UCRL 9453 (1960)
9. F. Fer, P. Lapostolle, C. Bieth, A. Cabrespine CERN MSC 018/999
10. D. Boussard Part. Acce. Confer. Washington March 1965 FF 18
11. L. Smith and R.L. Gluckstern Rev. Scient. Inst. 26, 220 (1955)
12. E. Martin Internal report (1965).

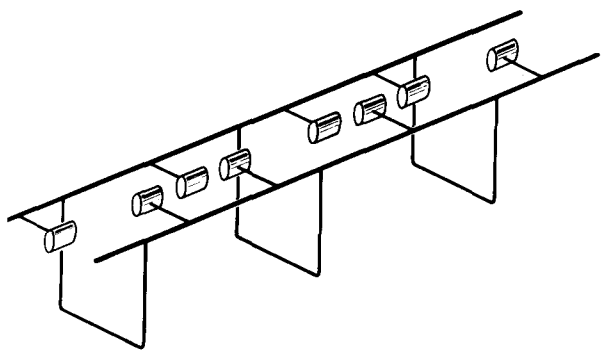

Fig. 1. Schematic view of the R.F. structure.

			Injector								C E V I L									
			$\frac{Z_i}{A} \geq 0.125$		$\frac{Z_i}{A} \geq 0.1$		$\frac{Z_i}{A} \geq 0.07$		$\beta = \frac{1\,MeV}{nucleon}$				$\beta = \frac{2\,MeV}{nucleon}$							
ELEMENT	Z	A	Z_i	Z_i/A	Z_i	Z_i/A	Z_i	Z_i/A	Z_i	Z_i/A	E MeV	β	Z_i	Z_i/A	E MeV	β	Z_i	Z_i/A	E MeV	β
Li	3	7	1+	0,143	1+	0,143	1+	0,143	3+	0,43	90	12,8	3+	0,43	90	12,8	3+	0,43	90	12,8
Be	4	10	2+	0,2	1+	0,1	1+	0,1	4+	0,4	112	11,2	4+	0,4	112	11,2	4+	0,4	112	11,2
B	5	11	2+	0,182	2+	0,182	1+	0,091	5+	0,455	159	14,5	5+	0,455	159	14,5	5+	0,455	159	14,5
C	6	12	2+	0,167	2+	0,167	1+	0,083	6+	0,5	210	17,5	6+	0,5	210	17,5	6+	0,5	210	17,5
N	7	14	2+	0,143	2+	0,143	1+	0,0715	7+	0,5	247,5	17,5	7+	0,5	247,5	17,5	7+	0,5	247,5	17,5
O	8	16	2+	0,125	2+	0,125	2+	0,125	7+	0,436	215	13,4	8+	0,5	280	17,5	8+	0,5	280	17,5
F	9	19	3+	0,158	2+	0,105	2+	0,105	8+	0,42	235	12,4	9+	0,474	298	15,7	9+	0,474	298	15,7
Ne	10	20	3+	0,15	2+	0,1	2+	0,1	8+	0,4	224	11,2	9+	0,45	283	14,15	9+	0,45	283	14,15
Na	11	23	3+	0,13	3+	0,13	2+	0,087	9+	0,39	246	10,7	10+	0,435	304	13,2	10+	0,435	304	13,2
Mg	12	24	3+	0,125	3+	0,125	2+	0,083	9+	0,375	236	9,85	10+	0,416	292	12,1	10+	0,416	292	12,1
Al	13	27	4+	0,148	3+	0,11	2+	0,074	10+	0,37	260	9,6	11+	0,408	314	11,6	11+	0,408	314	11,6
Si	14	28	4+	0,143	3+	0,107	2+	0,0715	10+	0,356	250	8,9	11+	0,392	302	10,8	11+	0,392	302	10,8
P	15	31	4+	0,129	4+	0,129	3+	0,0965	10+	0,322	226	7,3	12+	0,388	325	10,5	12+	0,388	325	10,5
S	16	32	4+	0,125	4+	0,125	3+	0,094	11+	0,343	264	8,25	12+	0,375	315	9,85	12+	0,375	315	9,85
Cl	17	35	5+	0,143	4+	0,114	3+	0,086	12+	0,343	288	8,2	13+	0,372	338	9,7	13+	0,372	338	9,7
A	18	40	5+	0,125	4+	0,1	3+	0,075	13+	0,325	295	7,4	14+	0,35	343	8,6	14+	0,35	343	8,6
K	19	39	5+	0,128	4+	0,102	3+	0,077	13+	0,334	304	7,6	15+	0,385	403	10,3	15+	0,385	403	10,3
Ca	20	40	5+	0,125	4+	0,1	3+	0,075	13+	0,325	295	7,4	16+	0,4	450	11,2	16+	0,4	450	11,2
Cu	29	63	8+	0,127	6+	0,095	5+	0,079	18+	0,286	360	5,7	20+	0,317	445	7,06	20+	0,317	445	7,06
Ge	32	74	10+	0,135	8+	0,108	6+	0,081	20+	0,27	378	5,1	22+	0,297	454	6,2	22+	0,297	454	6,2
Br	35	79	10+	0,126	8+	0,101	6+	0,076	20+	0,253	354	4,5	22+	0,278	430	5,45	22+	0,278	430	5,45
Kr	36	83	11+	0,132	8+	0,096	6+	0,072	21+	0,253	372	4,5	24+	0,29	488	5,88	24+	0,29	488	5,88

Fig. 4. Table I.

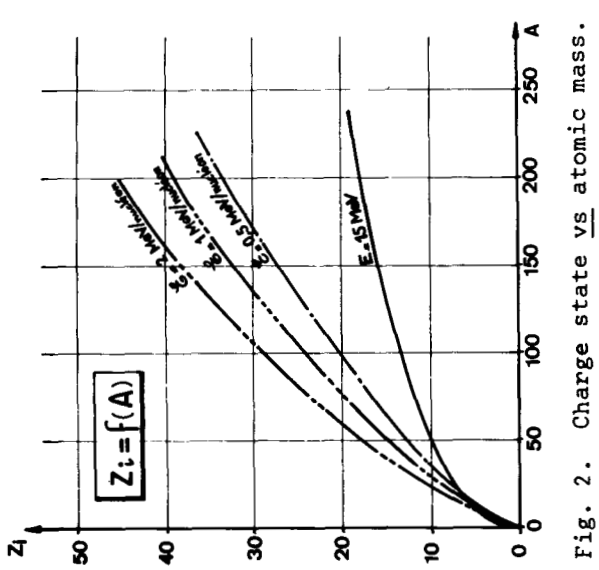

Fig. 2. Charge state vs atomic mass.

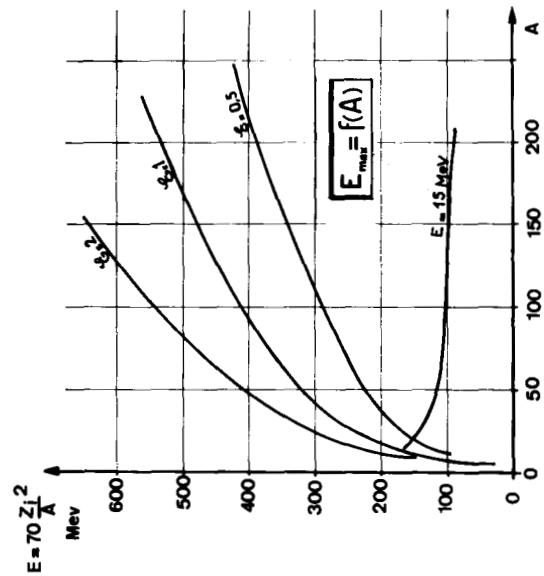

Fig. 3. Maximum energy vs atomic mass.

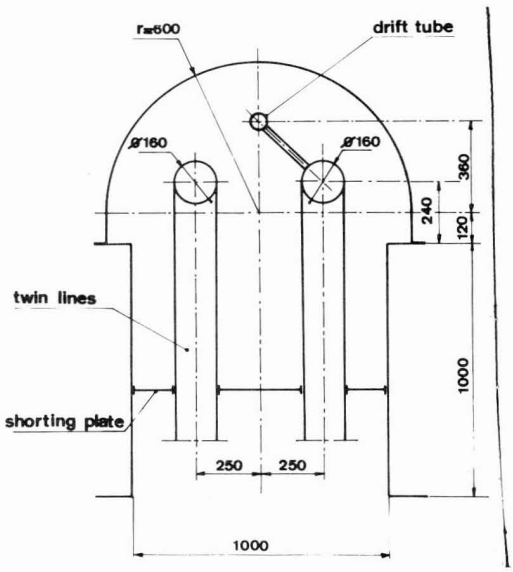

Fig. 5. Cross section of resonant line through the shorting plate.

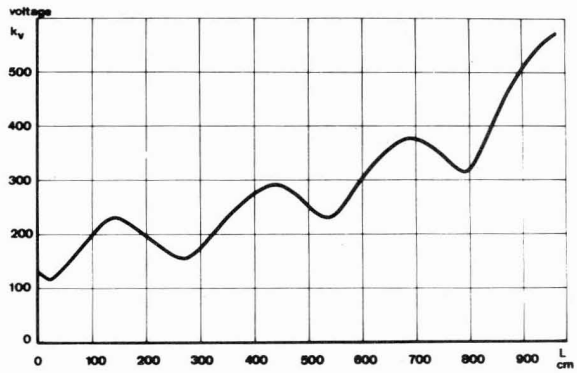

Fig. 6. Voltage distribution vs accelerator length.

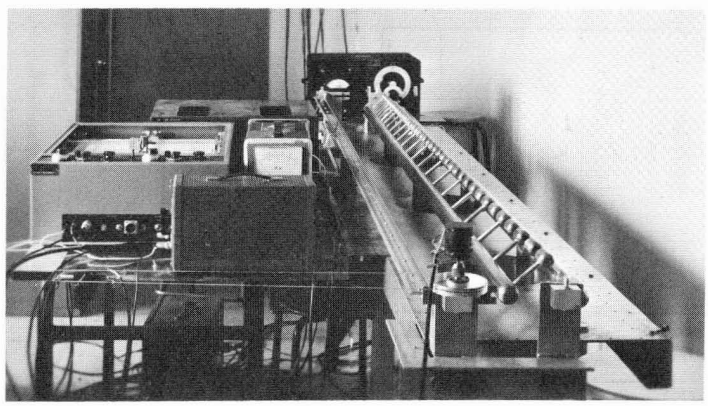

Fig. 7. View of the quarter scale RF structure model.

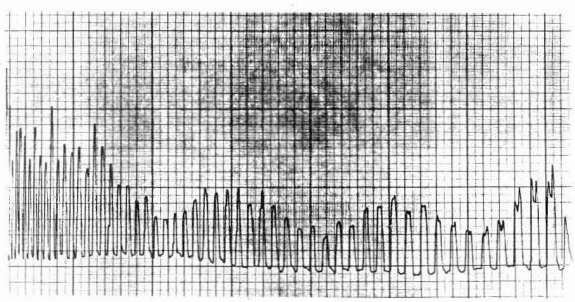

Fig. 8. Field measurement by perturbation method vs gap number.

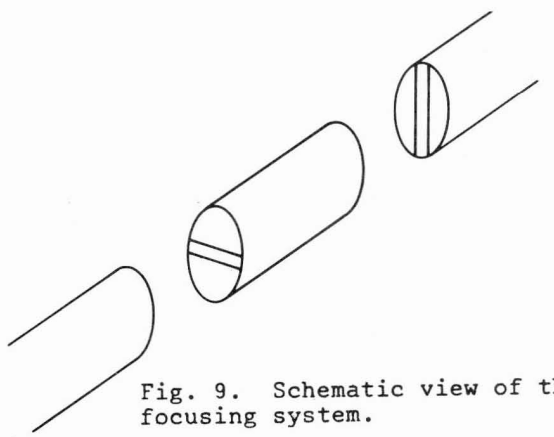

Fig. 9. Schematic view of the focusing system.

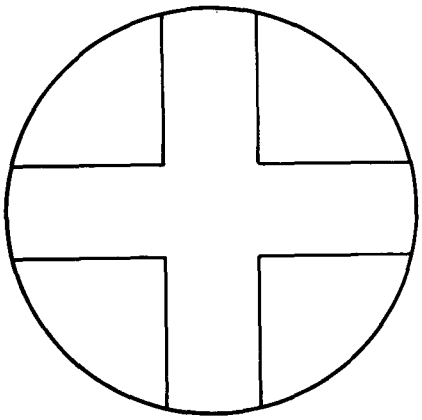

Fig. 10 Grids of Berkeley.

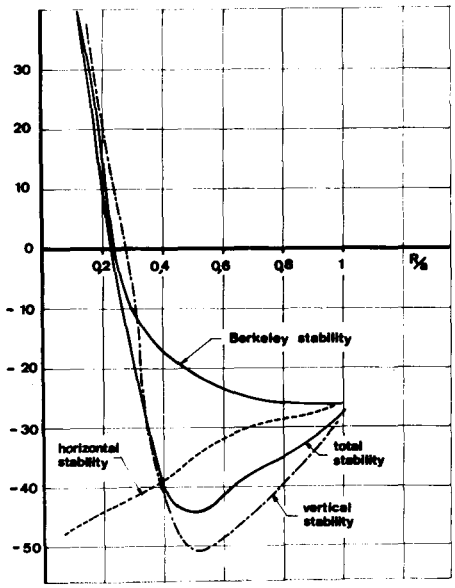

Fig. 11. Radial stability vs r/a for the grids of Berkeley and Orsay with g/L=1/2.5 and g/a=2.

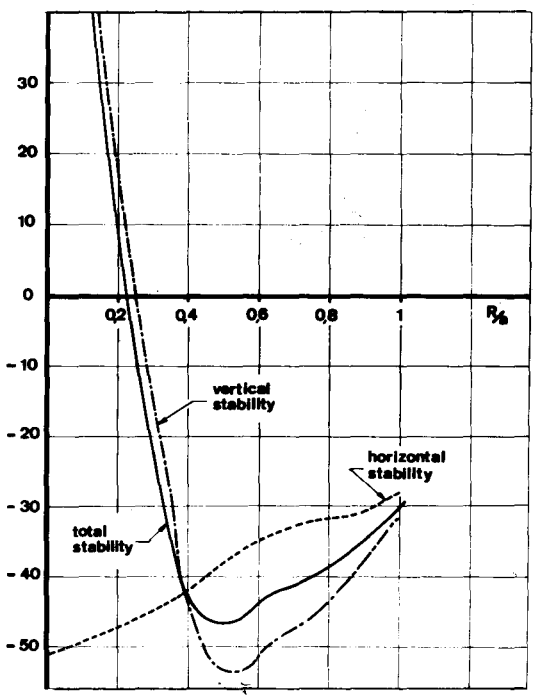

Fig. 12. Radial stability vs r/a for the grids of Orsay with g/L=1/2.7 and g/a=2.

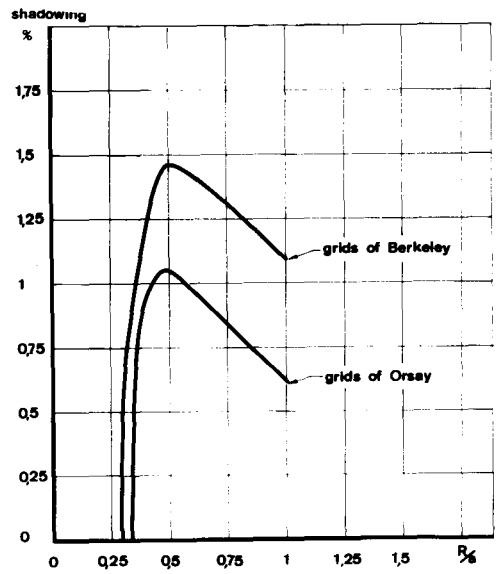

Fig. 13. Grids shadowing vs r/a.

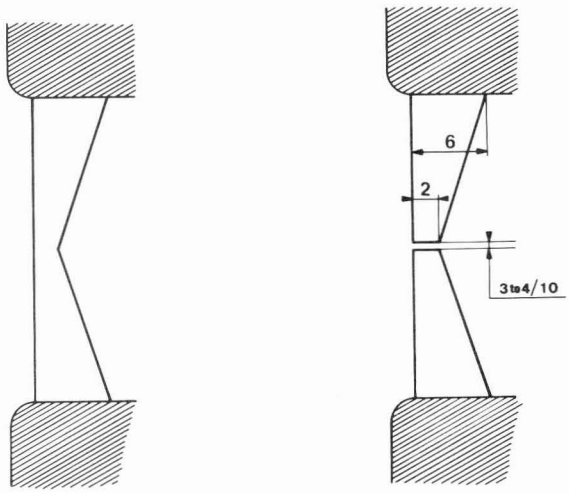

Fig. 14. Cross-section of grids.

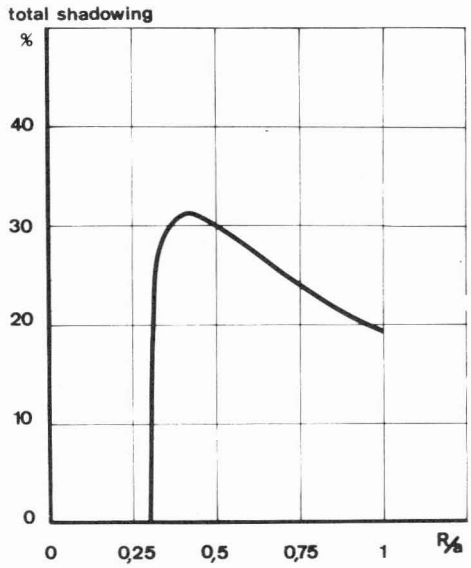

Fig. 15. Total shadowing vs r/a for 56 drift tubes.

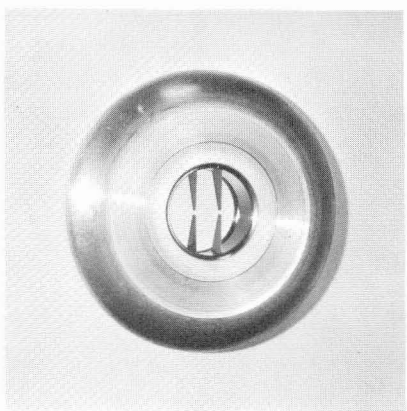

Fig. 16. View of grids.

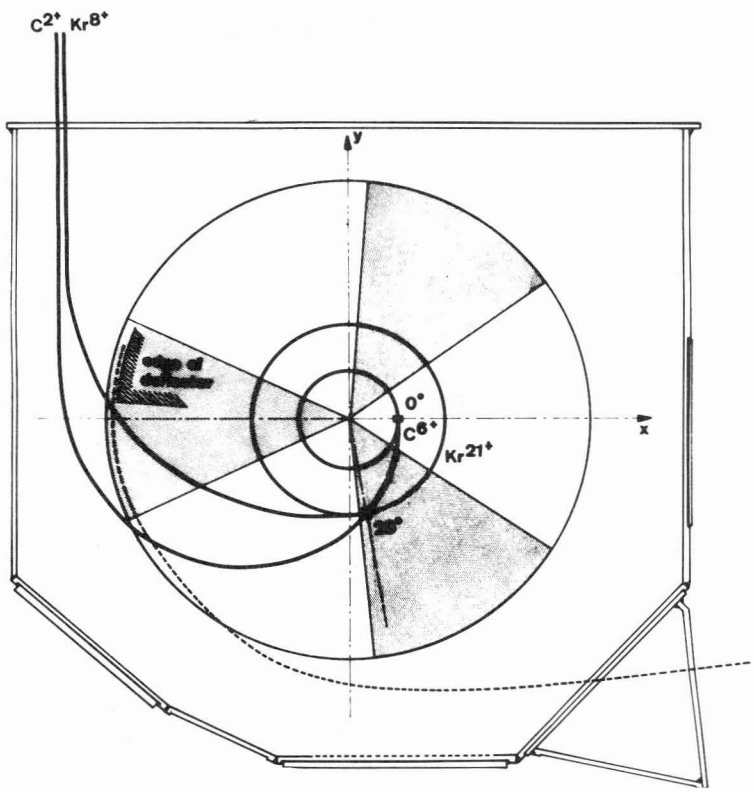

Fig. 17. Beam injection trajectories in the CEVIL with 14 Kgauss average field.

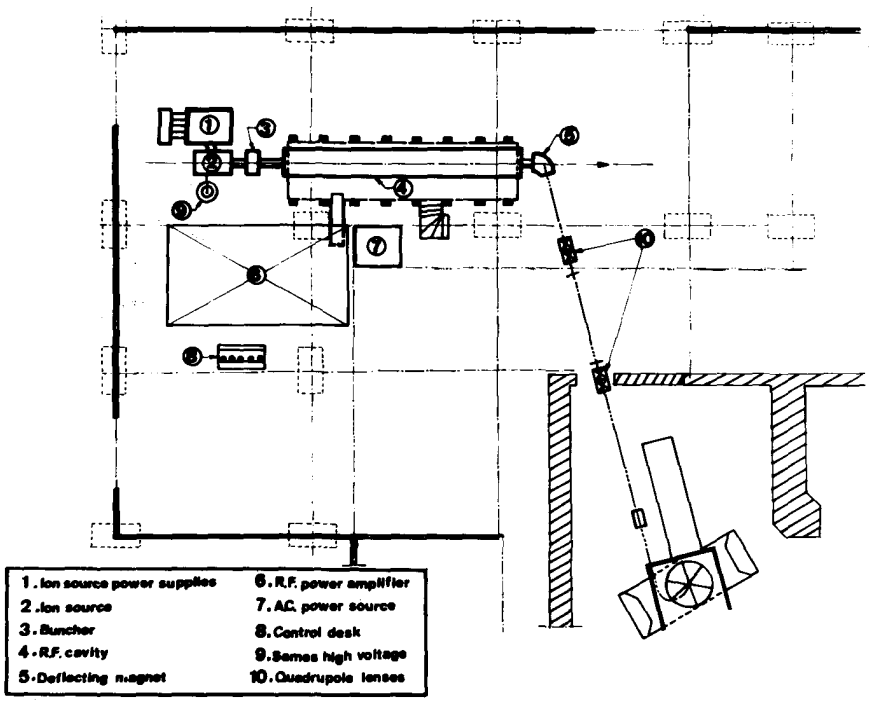

Fig. 18. Plan view of Hilac injector and CEVIL.

DISCUSSION

LIVINGOOD: Have you computed the vacuum which will be required in the CEVIL, in order that charge exchange will not rob you of your preciously acquired ions?

BIETH: Yes. We find that 1×10^{-7} vacuum is sufficient for good transmission efficiency in the linac, 10^{-6} in the cyclotron; for the linear accelerator we will probably use a turbo-molecular pump from SNEMCA.

LIVINGOOD: 1×10^{-7}, for xenon?

BIETH: Yes. Mr. Cabrespine made some calculations to find the efficiency for krypton. At our energies, I think the efficiency is quite good.

